

Experimental status of $b \rightarrow s\{\gamma, e^+e^-, \mu^+\mu^-\}$ at the LHC

Riley Henderson* on behalf of the LHCb, ATLAS, and CMS collaborations

School of Physics and Astronomy, Monash University

Wellington Road, Clayton VIC 3800, Australia

Department of Physics, University of Warwick,

Coventry CV4 7AL, United Kingdom

E-mail: riley.dylan.leslie.henderson@cern.ch

An overview of the status of measurements at the LHC on beauty hadron decays involving the $b \rightarrow s\{\gamma, e^+e^-, \mu^+\mu^-\}$ transitions is presented. Such decays are rare in the Standard Model and therefore particularly sensitive to potential New Physics contributions. Several anomalous measurements of $b \rightarrow s\ell^+\ell^-$ decay rates, with $\ell = \mu, e$, have sparked significant interest over the past decade, with hints of New Physics appearing in the effective couplings of leptons to the electroweak interaction. The presently available data continues to support this interpretation; however, recent precise results alter the picture in an important way and bring interesting new developments.

21st Conference on Flavor Physics and CP Violation (FPCP 2023)

29 May - 2 June 2023

Lyon, France

*Speaker

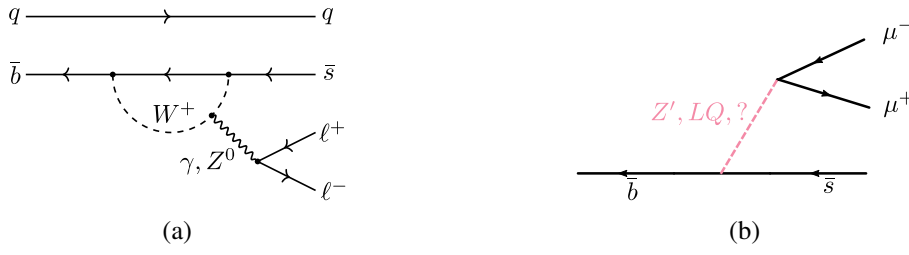


Figure 1: (a) The lowest order SM diagram for the $b \rightarrow s\ell^+\ell^-$ transition. (b) Possible NP contributions to the $b \rightarrow s\mu^+\mu^-$ transition.

1. Introduction

Flavour changing neutral current (FCNC) processes such as $b \rightarrow s\gamma$ and $b \rightarrow s\ell^+\ell^-$ are forbidden at tree level in the Standard Model (SM). They occur only at one-loop level or higher, for example, by the emission and reabsorption of a W boson as shown in Fig. 1a. This loop suppression leads to small predicted branching fractions, $\mathcal{B} \lesssim 10^{-5}$, allowing for the possibility of relatively large New Physics (NP) contributions, which may originate from mass scales far beyond that achievable in direct searches.

Interest in $b \rightarrow s\ell^+\ell^-$ decays was solidified following the start of the LHC era when the LHCb collaboration announced a series of anomalous experimental results in measurements of several exclusive $b \rightarrow s\ell^+\ell^-$ mediated decay channels. The first of the significant anomalies arose in the angular distribution of the decay $B^0 \rightarrow K^{*0}\mu^+\mu^-$, in which the LHCb measurement of the observable P'_5 was found to deviate from its SM prediction at the level of 3.7σ [1]. The P'_5 anomaly was confirmed in subsequent LHCb analyses with larger datasets [2, 3] and was followed by a procession of deviations in other $b \rightarrow s\ell^+\ell^-$ observables, including differential branching fractions [4–6] and ratios of branching fractions probing lepton flavour universality (LFU) [7, 8]. The growing set of anomalies was remarkably self-consistent, hinting towards a common explanation in terms of NP. Furthermore, measurements made by CMS and ATLAS of the same observables were found to be consistent with those of LHCb. In fact, global fits to all available measurements of $b \rightarrow s\ell^+\ell^-$ observables consistently showed a preference for LFU-violating NP in the effective $b \rightarrow s\mu^+\mu^-$ couplings. Possible explanations for this involve new heavy particles with masses at or above the electroweak scale. Examples include various incarnations of the leptoquark and Z' boson models shown in Fig. 1b, which can produce tree-level FCNCs.

Despite improvements in both theoretical and experimental precision, the $b \rightarrow s\ell^+\ell^-$ anomalies remain unresolved. The apparent deviations can in principle be accommodated for within the SM by larger than expected contributions from tree-level $b \rightarrow sq\bar{q}$ processes in which the $q\bar{q}$ pair annihilates leptonically [9], as illustrated in Fig. 2c. With this in mind, the experimental focus has been twofold: to further reduce uncertainties and to expand the set of observables available to test predictions. These efforts are also dedicated to the study of $b \rightarrow s\gamma$ observables which have shown no signs of anomalous experimental results thus far, but nonetheless provide crucial input to filter and constrain potential NP models. These proceedings review the current status of experimental results in $b \rightarrow s\{\gamma, e^+e^-, \mu^+\mu^-\}$ decays at the LHC.

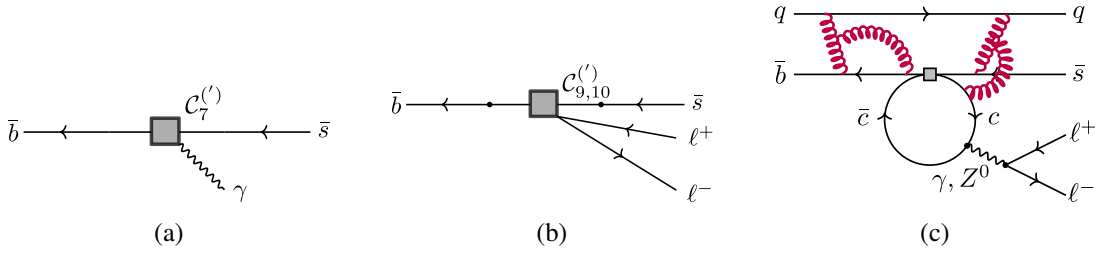


Figure 2: The SM WET description of the $b \rightarrow s\gamma$ and $b \rightarrow s\ell^+\ell^-$ transitions. (a) illustrates the effective operator \mathcal{O}_7 . (b) illustrates the effective operators \mathcal{O}_9 and \mathcal{O}_{10} . (c) illustrates the charm-loop contribution described by the non-local combination of operators $\mathcal{O}_{1,2}$ and J^μ , the electromagnetic current.

2. Theoretical overview

Decays involving a $b \rightarrow s$ transition are described within the SM Weak Effective Theory (WET) which is encapsulated by the following Hamiltonian,

$$\mathcal{H}_{\text{WET}} = \frac{-4G_F}{\sqrt{2}} V_{ts}^* V_{tb} \sum_i C_i^{(\prime)}(\mu) \mathcal{O}_i^{(\prime)}(\mu), \quad (1)$$

where: G_F is the Fermi constant; $V_{q'q}$ are elements of the Cabbibo-Kobayashi-Maskawa (CKM) matrix corresponding to the $q \rightarrow q'$ quark transition; the $\mathcal{O}_i^{(\prime)}$ are effective operators obtained by integrating out all heavy particles above the electroweak mass scale $\mu = M_W$; and the $C_i^{(\prime)}$ are the corresponding effective couplings, known as Wilson coefficients, which incorporate the dynamics of those heavy particles.

To obtain physical observables, one must calculate decay amplitudes via matrix elements of the form $\mathcal{A}(i \rightarrow f) = \langle f | \mathcal{H}_{\text{WET}} | i \rangle$. The values of the Wilson coefficients are obtained by equating the matrix element for a particular process calculated in the WET with that calculated in the full SM, *i.e.* $\langle f | \mathcal{H}_{\text{WET}} | i \rangle = \langle f | \mathcal{H}_{\text{SM}} | i \rangle$. Such matching calculations are performed at $\mu = M_W$ and then evolved down to the appropriate energy scale for the process, *i.e.* $\mu = m_b$, via renormalisation. In this approach, NP contributions manifest as shifts in the Wilson coefficients relative to their SM values.

The dominant contribution to $b \rightarrow s\gamma$ comes from the electromagnetic penguin operator, \mathcal{O}_7 , with a real photon as illustrated in Fig. 2a. Meanwhile, for $b \rightarrow s\ell^+\ell^-$, virtual photon contributions arise from \mathcal{O}_7 along with contributions from the electroweak penguin operators, \mathcal{O}_9 and \mathcal{O}_{10} , illustrated in Fig 2b. The relative contribution of each operator is dependent upon the squared invariant mass of the dilepton pair produced, $q^2 \equiv m_{\ell^+\ell^-}^2$. Important contributions from the four-quark operators \mathcal{O}_1 and \mathcal{O}_2 must also be accounted for, since the virtual $q\bar{q}$ pair produced can couple to a photon, as shown in Fig. 2c for the case of an internal charm quark loop. Such contributions create large enhancements in the decay rate for q^2 values close to a $q\bar{q}$ resonance mass, and greatly complicate theoretical calculations.

The main challenges in predicting $b \rightarrow s\ell^+\ell^-$ and $b \rightarrow s\gamma$ observables arise from the calculation of local and non-local form factors (FFs), which are q^2 dependent functions that parameterise the hadronic matrix elements. Theoretical efforts are most strongly concentrated on two main methods of calculation, known as lattice QCD and light-cone sum rules. These two approaches allow the

determination of the local FFs, whilst the more complex non-local FFs are typically related to the local FFs via an operator product expansion.

3. Experimental status

The relevant decay channels studied at the LHC fall into three main categories: fully leptonic, semi-leptonic, and radiative decays of b -quark hadrons. They each provide complementary sensitivity to the underlying WET parameters and are subject to different challenges and uncertainties, both experimentally and theoretically. In this section, the key observables studied in each type of decay are introduced and the latest experimental results are reviewed.

3.1 Fully leptonic decays

Thanks to their simplified hadronic structure, fully leptonic $b \rightarrow s\ell^+\ell^-$ decays are the cleanest theoretically; however, the set of available observables is limited. Moreover, they are the most suppressed in the SM, with branching fractions of the order of 10^{-9} or below, since B decays to pure dilepton final states are helicity suppressed in addition to the FCNC loop suppression. As a result, they are experimentally very challenging to analyse and results remain strongly dominated by statistical uncertainties.

The decay $B_s^0 \rightarrow \mu^+\mu^-$ is a well known example and constitutes one of the flagship B physics measurements performed at the LHC. In the SM, the branching fraction has a predicted value of $\mathcal{B}(B_s^0 \rightarrow \mu^+\mu^-)_{\text{SM}} = (3.2 \pm 0.2) \times 10^{-9}$ [10]; however, measurements of this quantity are convoluted by B_s^0 - \bar{B}_s^0 mixing effects, especially in the presence of very low statistics. Experimentally, the minuscule signal rate currently prohibits the use of flavour tagging information, meaning that measurements are made without distinguishing between B_s^0 and \bar{B}_s^0 . Predictions for the experimentally measured branching fraction therefore require a correction relative to the theoretical $B_s^0 \rightarrow \mu^+\mu^-$ branching fraction to account for the difference in decay widths between the B_s^0 mass eigenstates [11]. Applying this correction results in a 14% increase, giving a predicted experimental branching fraction of $\mathcal{B}(B_s^0 \rightarrow \mu^+\mu^-)_{\text{exp,SM}} = (3.66 \pm 0.14) \times 10^{-9}$ [12].

In comparing the predicted branching fraction to experiment, consideration must be given to the fact that potential NP contributions can affect the measured result either directly through the $B_s^0 \rightarrow \mu^+\mu^-$ decay itself, or via the mixing. Potential ambiguities can be resolved through the decay time distribution, which gives complementary access to the parameters of the mixing correction. In particular, a measurement of both the branching fraction and the effective lifetime, defined as

$$\tau_{\mu^+\mu^-} \equiv \frac{\int_0^\infty t \Gamma(B_s^0(t) \rightarrow \mu^+\mu^-) dt}{\int_0^\infty \Gamma(B_s^0(t) \rightarrow \mu^+\mu^-) dt}, \quad (2)$$

allows one to distinguish NP contributions to the decay from B_s^0 - \bar{B}_s^0 mixing effects [13]. Alternatively, NP can modify the effective lifetime whilst conspiring to keep the branching fraction unchanged. Under the assumption of negligible CP violation in the B_s^0 - \bar{B}_s^0 mixing, as expected in the SM, only the heavy B_s^0 mass eigenstate can decay to two muons [14]; this gives an expected effective lifetime of $\tau_{\mu^+\mu^-,\text{SM}} = \tau_{B_H} = 1.624 \pm 0.009$ [15].

The 2020 combination of measurements made by ATLAS [16], CMS [17], and LHCb [18], shown in Fig. 3, resulted in an average value of the $\mathcal{B}(B_s^0 \rightarrow \mu^+\mu^-) = (2.69_{-0.35}^{+0.37}) \times 10^{-9}$ [19].

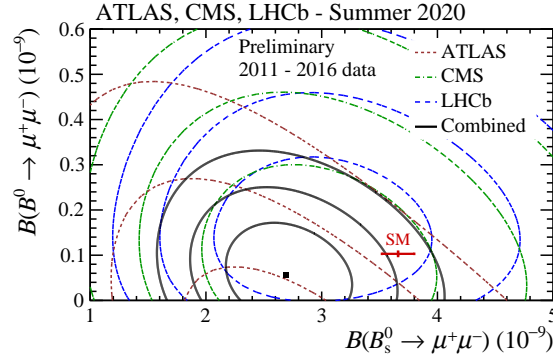


Figure 3: Likelihood contours shown in the plane of the $B_s^0 \rightarrow \mu^+\mu^-$ and $B^0 \rightarrow \mu^+\mu^-$ branching fractions for measurements made by the ATLAS [16], CMS [17], and LHCb [18] collaborations along with their combination. This figure shows the results of the 2020 combination [19] which was compatible with the SM within 2.1σ .

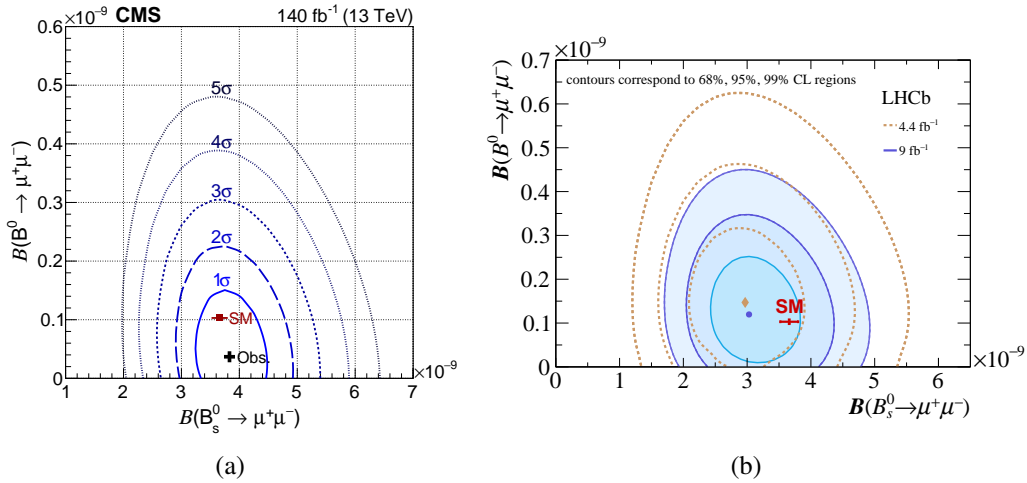


Figure 4: Likelihood contours shown in the plane of the $B_s^0 \rightarrow \mu^+\mu^-$ and $B^0 \rightarrow \mu^+\mu^-$ branching fractions for updated measurements made by the (a) CMS [17], and (b) LHCb [18] collaborations.

These measurements were performed as a simultaneous search for $B^0 \rightarrow \mu^+\mu^-$, proceeding through the further CKM suppressed $b \rightarrow d\ell^+\ell^-$ transition. In the 2D plane of $B_s^0 \rightarrow \mu^+\mu^-$ and $B^0 \rightarrow \mu^+\mu^-$ branching fractions, the results of the combination were compatible with the SM within 2.1σ . The small tension was later eradicated following updated measurements from LHCb [14] and CMS [20] in 2022, shown in Fig. 4. Whilst an official update of the LHC combination still awaits, an unofficial combination including the new LHCb and CMS measurements resulted in $\mathcal{B}(B_s^0 \rightarrow \mu^+\mu^-) = (3.52^{+0.32}_{-0.30}) \times 10^{-9}$ [21], in agreement with the SM within 0.4σ . In these latest analyses, LHCb and CMS both also measured the effective lifetime and obtained values of $\tau_{\mu^+\mu^-} = 2.07 \pm 0.29$ (stat.) ± 0.03 (syst.) ps and $\tau_{\mu^+\mu^-} = 1.83^{+0.23}_{-0.20}$ (stat.) $^{+0.04}_{-0.04}$ (syst.) ps, respectively. The LHCb and CMS results are consistent with τ_{BH} at 1.5σ and 1σ , respectively.

Searches have been performed for several other related decays which could expand the set of available observables in fully leptonic decays. For example, the decay $B_s^0 \rightarrow e^+e^-$ has a SM

branching fraction that is a further 5 orders of magnitude suppressed, at $\mathcal{B}(B_s^0 \rightarrow e^+e^-)_{\text{SM}} = (8.60 \pm 0.36) \times 10^{-14}$ [12], due to an enhancement of the helicity suppression by the tiny electron mass. Also of interest are decays in which the B_s^0 meson radiates an additional photon, leading to final states with either four leptons in the virtual case, e.g. $B_s^0 \rightarrow \mu^+\mu^-\mu^+\mu^-$, or the radiative-leptonic decay $B_s^0 \rightarrow \mu^+\mu^-\gamma$ in the real case. The additional final state particles lift the helicity suppression, giving them comparable branching fractions to the dimuon final states. The $B_s^0 \rightarrow \mu^+\mu^-\gamma$ decay was searched for in the range $m_{\mu\mu} > 4.9 \text{ GeV}/c^2$ by LHCb in their most recent simultaneous $B_{(s)}^0 \rightarrow \mu^+\mu^-$ fit; meanwhile, dedicated LHCb analyses were performed to search for the dielectron and four-muon final states. No evidence for any of these decays was found and the following limits were placed on the branching fractions at 95% confidence level [14, 22, 23]:

$$\begin{aligned}\mathcal{B}(B_s^0 \rightarrow \mu^+\mu^-\gamma) &< 2.0 \times 10^{-9}, \\ \mathcal{B}(B_s^0 \rightarrow e^+e^-) &< 11.2 \times 10^{-9}, \\ \mathcal{B}(B_s^0 \rightarrow \mu^+\mu^-\mu^+\mu^-) &< 8.6 \times 10^{-10}.\end{aligned}$$

3.2 Semi-leptonic decays

Semi-leptonic $b \rightarrow s\ell^+\ell^-$ decays typically have branching fractions of the order of 10^{-6} and yield much higher statistics relative to the fully leptonic modes. Semi-leptonic final states also contain more degrees of freedom, giving access to a richer set of observables. However, they suffer from larger theoretical uncertainties due to the presence of both intermediate and final state hadrons. These effects are most prominent in the q^2 regions close to the narrow $q\bar{q}$ resonances; hence, measurements are typically made in bins of q^2 , with the three bins corresponding to the $\phi(1020)$, J/ψ , and $\psi(2S)$ resonances explicitly vetoed. In the subsections below, experimental results are split into three categories of observables which carry varying levels of dependence on this hadronic pollution.

3.2.1 Branching fractions

Shown in Fig. 5 are the differential branching fractions of several semi-leptonic $b \rightarrow s\ell^+\ell^-$ decays measured as a function of q^2 —all of which appear to show an interesting disagreement between experiment and theory in the low to central q^2 range, $1 < q^2 < 8 \text{ GeV}^2/c^4$. The $B_s^0 \rightarrow \phi\mu^+\mu^-$ branching fraction measured by LHCb [6] (Fig. 5a) was found to deviate by 3.6σ from its SM prediction across the $1.1 < q^2 < 6.0 \text{ GeV}^2/c^4$ region, based on calculations from Ref. [24]. Similar patterns have been identified in the branching fractions of other decays measured by LHCb, including $B \rightarrow K^{(*)}\mu^+\mu^-$ [4, 5, 8, 25–27] and $\Lambda_b^0 \rightarrow \Lambda^{(*)}\mu^+\mu^-$ [28, 29]. Moreover, several of these branching fractions have also been studied by other experiments both at the LHC and elsewhere, including CMS [30], Belle [31, 32], BaBar [33], and CDF [34], with all results found to be compatible with those of LHCb. Following recent improvements in theoretical calculations, the largest tension is currently observed in the $B^+ \rightarrow K^+\mu^+\mu^-$ channel (Fig. 5c) in which the LHCb measurements deviate from the SM predictions at greater than 4σ in several bins at central q^2 [35]. These deviations are found to be significantly reduced upon considering NP shifts of $\Delta C_9 \approx -1.0$, and $\Delta C_{10} \approx +0.4$, relative to the SM predictions [36, 37]. However, branching fractions are the most sensitive to the hadronic physics and the quoted tensions and optimal NP shifts depend closely on the choice of form factors and power corrections.

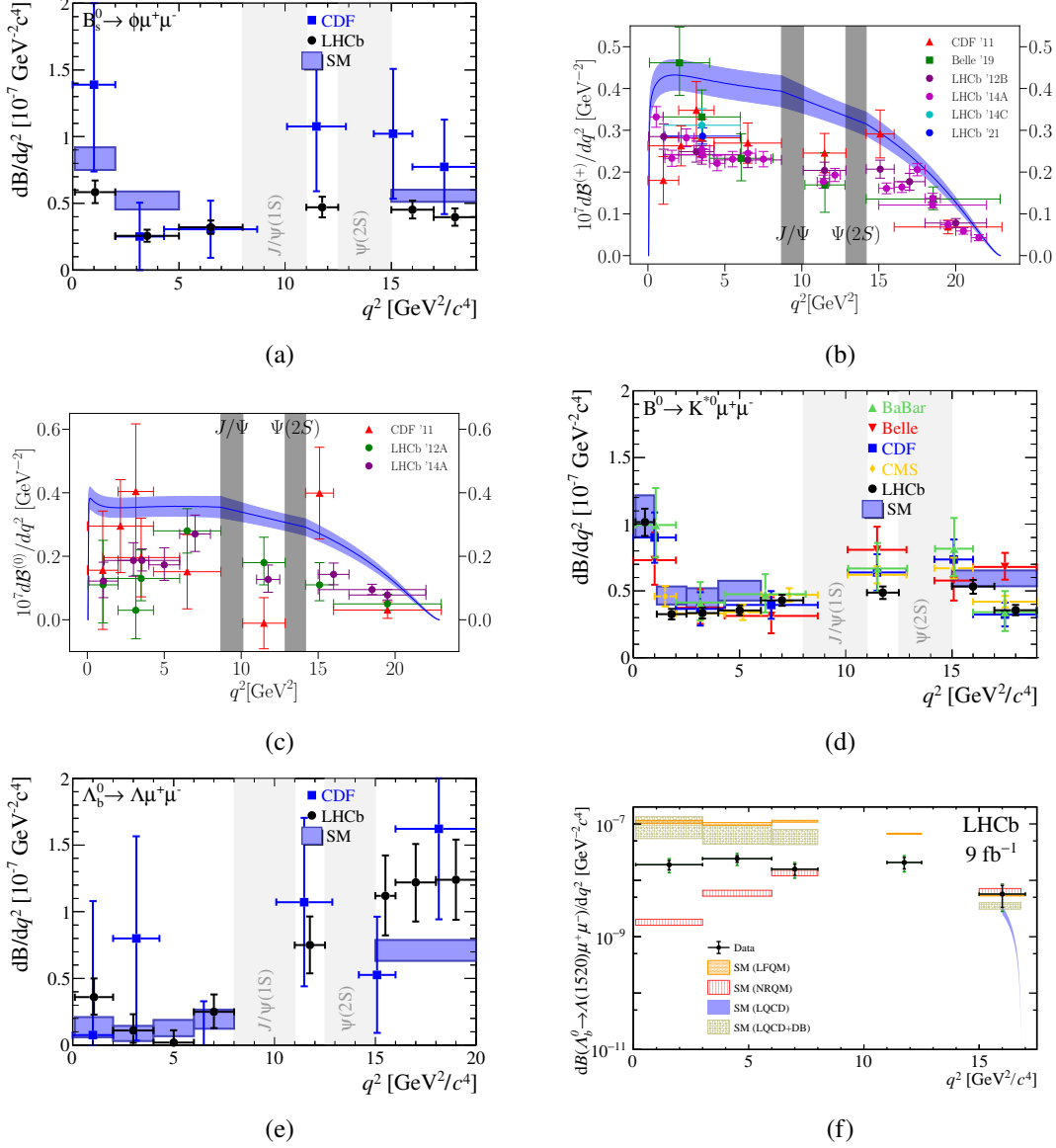


Figure 5: Differential branching fraction measurements of the semi-leptonic $b \rightarrow s\ell^+\ell^-$ decays: (a) $B_s^0 \rightarrow \phi\mu^+\mu^-$, (b) $B^+ \rightarrow K^+\mu^+\mu^-$, (c) $B^0 \rightarrow K_S^0\mu^+\mu^-$, (d) $B^0 \rightarrow K^{*0}\mu^+\mu^-$, (e) $\Lambda_b^0 \rightarrow \Lambda\mu^+\mu^-$, and (f) $\Lambda_b^0 \rightarrow \Lambda(1520)\mu^+\mu^-$. Experimental results are shown for CDF [34], Belle [31, 32], BaBar [33], CMS [30], and LHCb [4–6, 8, 26, 28, 29]; theoretical predictions are obtained from Refs. [24, 36, 38–44]. Figs. (a), (d), and (e) were obtained from Ref. [45], whilst Figs. (b) and (c) were obtained from Ref. [36].

3.2.2 Angular distributions

The angular distributions of $b \rightarrow s\ell^+\ell^-$ decays provide access to a large number of additional observables that are complementary to the branching fractions in terms of both sensitivity to NP and dependence on hadronic interactions. They are typically expressed as a function of the invariant masses and helicity angles of the final state particles in the decay. For example, considering the decay $B \rightarrow V\ell^+\ell^-$, where V is a vector meson decaying to, e.g. $K^+\pi^-$, one can write the decay rate as

$$\frac{d^4\bar{\Gamma}}{dq^2 d^3\bar{\Omega}} = \frac{9}{32\pi} \sum_i \bar{J}_i(q^2) f_i(\cos\theta_\ell, \cos\theta_K, \phi), \quad (3)$$

and likewise for $\bar{B} \rightarrow \bar{V}\ell^+\ell^-$, with $\bar{J}_i \rightarrow J_i$ and $\bar{\Gamma} \rightarrow \Gamma$. In the above, $\bar{\Omega} \equiv (\cos\theta_\ell, \cos\theta_K, \phi)$, θ_K (θ_ℓ) denotes the angle of the K^+ (μ^+) with respect to the direction of flight of the B meson in the rest frame of the V ($\mu^+\mu^-$), and ϕ denotes the angle between the $\mu^+\mu^-$ and V decay planes in the rest frame of the B meson. A set of CP -averaged and CP -asymmetry observables can then be defined, respectively, as

$$S_i = \frac{1}{d(\Gamma + \bar{\Gamma})/dq^2} (J_i + \bar{J}_i), \quad (4)$$

$$A_i = \frac{1}{d(\Gamma + \bar{\Gamma})/dq^2} (J_i - \bar{J}_i). \quad (5)$$

From these, it is commonplace to take ratios between certain observables in order to form so called *optimised* angular observables, $P_i^{(\prime)}$, which benefit from some cancellation in hadronic form factor uncertainties [46].

The CP -averaged P-wave angular distribution of the decay $B^0 \rightarrow K^{*0}\mu^+\mu^-$ is the most extensively studied at the LHC and consists of the observables S_{1-9} . Measurements of the angular observables are found to be in generally good agreement with SM predictions. However, Fig. 6a shows a series of measurements made by the LHCb [3], CMS [47], ATLAS [48], and Belle [49] collaborations of the optimised observable $P'_5 \equiv S_5/\sqrt{F_L(1-F_L)}$, where $F_L \equiv S_{1c}$ ¹ is the fraction of longitudinal polarisation of the K^{*0} meson. A deviation from the SM predictions of Refs. [50,51] is evident in the bins covering the range $q^2 \in [4, 8] \text{ GeV}^2/c^4$, which appears consistent across experiments. Further support for the P'_5 anomaly was provided by the LHCb measurement using the isospin partner decay $B^+ \rightarrow K^{*+}\mu^+\mu^-$, shown in Fig. 6b, which exhibits a similar tension in the central q^2 bins [52]. Interestingly, a larger discrepancy was found in the optimised observable $P_2 \equiv \frac{2}{3}A_{\text{FB}}/(1-F_L)$, where $A_{\text{FB}} \equiv \frac{3}{4}S_{6s}$ is the forward-backward asymmetry of the dimuon system. A reduced $B^+ \rightarrow K^{*+}\mu^+\mu^-$ angular distribution was also studied by CMS, in which measurements of the forward-backward asymmetry A_{FB} and F_L were found to be in good agreement with the SM and compatible with the LHCb measurements [53]. Considering all observables, the LHCb measurements of the CP -averaged $B \rightarrow K^{(*)}\mu^+\mu^-$ angular distributions both collectively favour a NP contribution of $\Delta C_9 \approx -1.0$ over the SM.

Angular analyses have additionally been performed for several other semi-leptonic $b \rightarrow s\ell^+\ell^-$ decay channels, including $B_s^0 \rightarrow \phi\mu^+\mu^-$ [54,55], $B \rightarrow K\mu^+\mu^-$ [56,57], and $\Lambda_b^0 \rightarrow \Lambda\mu^+\mu^-$ [58].

¹The subscript c (s) on some of the CP -averaged angular observables indicates that the observable carries a $\cos^2\theta_K$ ($\sin^2\theta_K$) dependence.

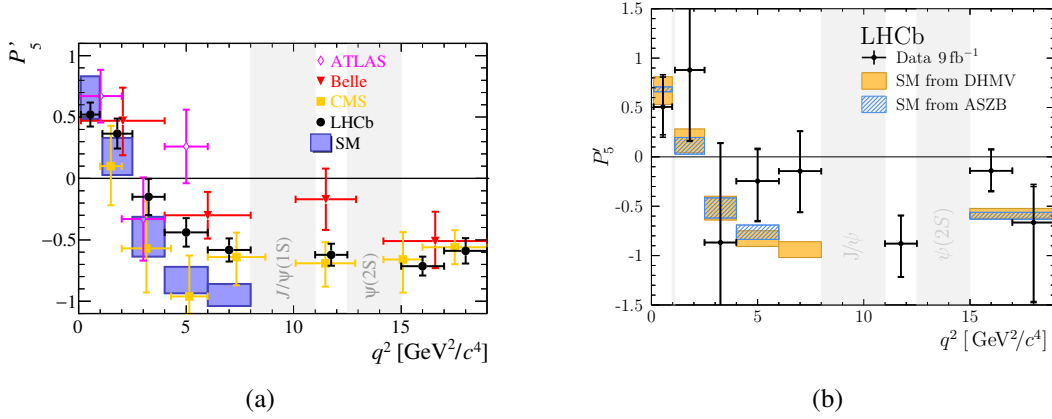


Figure 6: Comparison of measurements and theoretical predictions for the optimised angular observable P_5' for the decays (a) $B^0 \rightarrow K^{*0}\mu^+\mu^-$ (figure obtained from Ref. [45]) and (b) $B^+ \rightarrow K^{*+}\mu^+\mu^-$. Experimental results are shown for ATLAS [48], CMS [47], LHCb [3,52], and Belle [49]. The anomaly at central q^2 appears in both decay modes and is largely consistent between the measurements made by different experiments.

The results of these measurements are largely in good agreement with the SM. However, the CP -averaged $B_s^0 \rightarrow \phi\mu^+\mu^-$ observables also collectively favour a NP shift of $\Delta C_9 \approx -1.0$. Only a subset of the CP -averaged observables are accessible in the $B_s^0 \rightarrow \phi(\rightarrow K^+K^-)\mu^+\mu^-$ decay, since it is not flavour-specific and requires a slightly different angular convention. In particular, in the untagged decay rate, the CP -averaged observables $S_{5,6,8,9}$ are replaced by their CP -asymmetry counterparts $A_{5,6,8,9}$. The latter offer little sensitivity to C_9 , but provide unique sensitivity to potential NP sources of CP violation, without the need for flavour tagging [59]. The different spin structures of the $B \rightarrow K\mu^+\mu^-$ and $\Lambda_b^0 \rightarrow \Lambda\mu^+\mu^-$ decays also result in a different set of angular observables — therefore, these three decays expand the breadth of available SM tests significantly and are consistent with the preference for NP in C_9 observed in the $B \rightarrow K^{(*)}\mu^+\mu^-$ modes.

3.2.3 Lepton flavour universality ratios

Ratios of branching fractions of the form

$$R_X = \frac{\mathcal{B}(B \rightarrow X\mu^+\mu^-)}{\mathcal{B}(B \rightarrow Xe^+e^-)} \bigg/ \frac{\mathcal{B}(B \rightarrow XJ/\psi(\rightarrow \mu^+\mu^-))}{\mathcal{B}(B \rightarrow XJ/\psi(\rightarrow e^+e^-))}, \quad (6)$$

are used to test LFU — a central assumption of the SM flavour sector. The R_X ratios are among the cleanest observables available in $b \rightarrow s\ell^+\ell^-$ decays, since all hadronic effects cancel in the ratio and theoretical uncertainties are curbed at the 1% level. Any true deviation from unity would therefore point unambiguously towards LFU-violating NP. They are designed to be robust against the mismodelling of muon/electron detection efficiencies by means of the double ratio approach, in which the FCNC mode ratios are normalised to the ratio of the corresponding tree-level decays passing through the J/ψ resonance. The latter have the same decay topology, which facilitates the cancellation of several sources of experimental systematic uncertainties, and LFU is well established in these decays.

Until recently, LHCb measurements of the R_X ratios for several different final states, shown in Fig. 7a, had been found to deviate from their SM predictions [7, 8, 60, 61]. The most significant

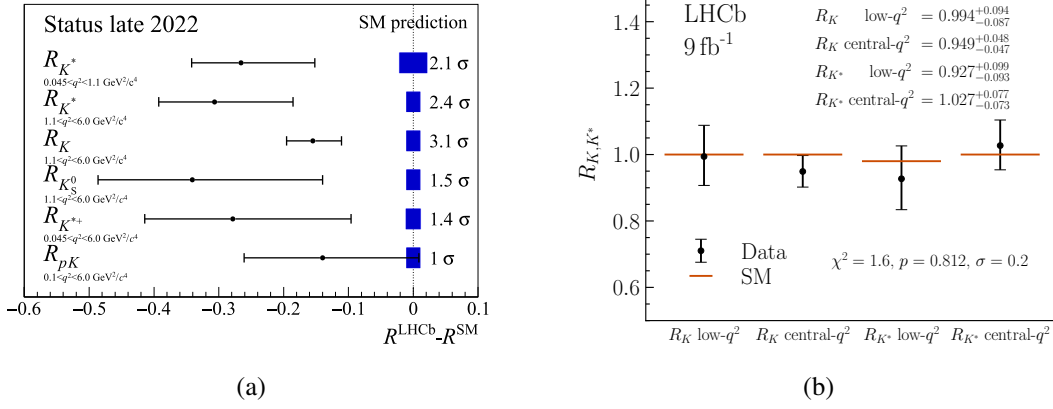


Figure 7: The status of LFU measurements made by the LHCb collaboration. (a) shows the results the prior to December 2022 for the decays $R_{K^{*0}}$ [7], R_K [8], $R_{K_S^0}$ [60], $R_{K^{*+}}$ [60], and R_{pK} [61]. (b) shows the recent updates of R_K and R_{K^*} [62, 63].

deviation appeared in R_K , where a 3.1σ tension was evident in the central q^2 bin, defined as range $1.1 < q^2 < 6.0 \text{ GeV}^2/c^4$. However, this measurement was recently reperformed in a simultaneous determination of R_K and $R_{K^{*0}}$, which led to markedly different results [62, 63], as shown in Fig. 7b. The difference in results for $R_{K^{*0}}$ is mostly statistical, whilst for R_K the difference is a combination of statistical and systematic effects. The updated and improved measurement differs in two main ways, with the first being the use of more stringent particle identification (PID) criteria to reduce the level of misidentified backgrounds which can mimic the signal — particularly those affecting the final states containing electrons. Secondly, the residual misidentified backgrounds in the electron modes that escaped the tighter PID criteria were explicitly accounted for using a new data driven inclusive modelling technique. The new measurement represents the most precise test of LFU performed in $b \rightarrow s\ell^+\ell^-$ decays, and the results are compatible with LFU conservation within 0.2σ .

3.3 Radiative decays

Radiative decays involving the $b \rightarrow s\gamma$ transition share the same hadronic structure as $b \rightarrow s\ell^+\ell^-$ decays and have branching fractions of the order of 10^{-5} . They are dominated by contributions from $O_7^{(\prime)}$ and represent sensitive probes of the polarisation structure of the weak interaction. The chiral $V - A$ formulation of the latter implies that the photons emitted in $\bar{b} \rightarrow \bar{s}\gamma$ transitions are predominantly left(right)-handed, with the chirality flipped decays suppressed according to the relation $C_7' = \frac{m_s}{m_b} C_7$. However, this relation can be subject to large NP modification in models involving right-handed currents. Such possibilities can be tested in the radiative and semi-leptonic decays of b hadrons.

The time-dependent rate for the flavour-nonspecific decay $\bar{B}_q^0 \rightarrow M\gamma$, can be written as [64]

$$\Gamma(t) \propto e^{-\Gamma_q t} \left[\cosh(\Delta\Gamma_q t/2) - A^\Delta \sinh(\Delta\Gamma_q t/2) + \zeta C \cos(\Delta m_q t) - \zeta S \sin(\Delta m_q t) \right] \quad (7)$$

where $\zeta = 1$ (-1) for an initial B_q^0 (\bar{B}_q^0). The rate above depends on the mass and width differences, Δm_q and $\Delta\Gamma_q$, between the flavour eigenstates of the B_q^0 meson, and three other observables — A^Δ ,

C , and S . The coefficient C is a measure of direct CP violation in the decay, whilst A^Δ and S carry sensitivity to the photon polarisation and arise only through mixing between the B_q^0 meson flavour eigenstates, hence the requirement of a flavour-nonspecific final state.

Unfortunately, A^Δ is virtually inaccessible in $\overline{B^0}$ decays due to the negligible decay width difference $\Delta\Gamma_d$. Moreover, the reconstruction of neutral particles at LHCb is challenging, thus the requirement of a flavour-nonspecific final state in, *e.g.* $B^0 \rightarrow K^{*0}\gamma$, is impractical as it requires reconstructing $K^{*0} \rightarrow K_S^0\pi^0$. The decay $B_s^0 \rightarrow \phi\gamma$ with $\phi \rightarrow K^+K^-$, on the other hand, circumvents both of these issues and was studied by LHCb using Run 1 data, which led to the following results [65],

$$\begin{aligned} A_{\phi\gamma}^\Delta &= -0.67_{-0.41}^{+0.37} \text{ (stat.)} \pm 0.17 \text{ (syst.)}, \\ C_{\phi\gamma} &= 0.11 \pm 0.29 \text{ (stat.)} \pm 0.11 \text{ (syst.)}, \\ S_{\phi\gamma} &= 0.43 \pm 0.30 \text{ (stat.)} \pm 0.11 \text{ (syst.)}. \end{aligned}$$

These measurements are in good agreement with the SM predictions of Ref. [64]. A direct CP asymmetry measurement was also performed by LHCb on the decay $B^0 \rightarrow K^{*0}\gamma$ with $K^* \rightarrow K^+\pi^-$ in which the results were consistent with no asymmetry [66].

Angular distributions in $b \rightarrow s\ell^+\ell^-$ decays also provide excellent sensitivity to the photon polarisation, specifically in the region of low q^2 where the decay rate is dominated by virtual photon contributions from $C_7^{(\prime)}$. Isolating the $C_7^{(\prime)}$ dominated part of the dilepton spectrum necessitates looking at $b \rightarrow se^+e^-$ modes, since the kinematic threshold to produce a dimuon pair forbids access to sufficiently low q^2 values. In the decay $B^0 \rightarrow K^{*0}e^+e^-$, two of the angular observables, denoted $A_T^{(2)}$ and A_T^{Im} , are sensitive to the $b \rightarrow s\gamma$ photon polarisation in the $q^2 \rightarrow 0$ limit. They are related to the optimised angular observables described in Sec. 3.2.2 by $A_T^{(2)} \equiv P_1$ and $A_T^{\text{Im}} \equiv -2P_3^{CP}$. An angular analysis of the $B^0 \rightarrow K^{*0}e^+e^-$ decay was performed by LHCb in the range $0.0008 < q^2 < 0.257 \text{ GeV}^2/c^4$, resulting in the measured values [67]

$$\begin{aligned} A_T^{(2)} &= +0.11 \pm 0.10 \text{ (stat.)} \pm 0.02 \text{ (syst.)}, \\ A_T^{\text{Im}} &= +0.02 \pm 0.10 \text{ (stat.)} \pm 0.01 \text{ (syst.)}. \end{aligned}$$

These results are also in good agreement with SM predictions, showing no signs of NP enhancement of right-handed photons in $b \rightarrow s\gamma$.

A measurement of the photon polarisation is also possible via the angular distribution of radiative baryonic decays such as $\Lambda_b^0 \rightarrow \Lambda\gamma$. The polarisation parameter $\alpha_\gamma \equiv (\gamma_L - \gamma_R)/(\gamma_L + \gamma_R)$, where γ_L and γ_R represent the number of left- and right-handed photon emissions, features directly in the $\Lambda_b^0 \rightarrow \Lambda\gamma$ differential decay rate. An angular analysis of this decay was performed by LHCb, wherein they measured [68]

$$\alpha_\gamma = 0.82_{-0.26}^{+0.17} \text{ (stat.)}_{-0.13}^{+0.04} \text{ (syst.)},$$

in concordance with the SM expectation of $\alpha_\gamma = 1$ within 1σ . In the same analysis, LHCb also determined the polarisation parameter separately for the $\Lambda_b^0 \rightarrow \Lambda\gamma$ and $\overline{\Lambda}_b^0 \rightarrow \overline{\Lambda}\gamma$ samples and found the results to be consistent with CP conservation. A search for the decay $\Xi_b^- \rightarrow \Xi^0\gamma$ was also performed by LHCb; no signal was observed, allowing an upper limit to be set on the branching

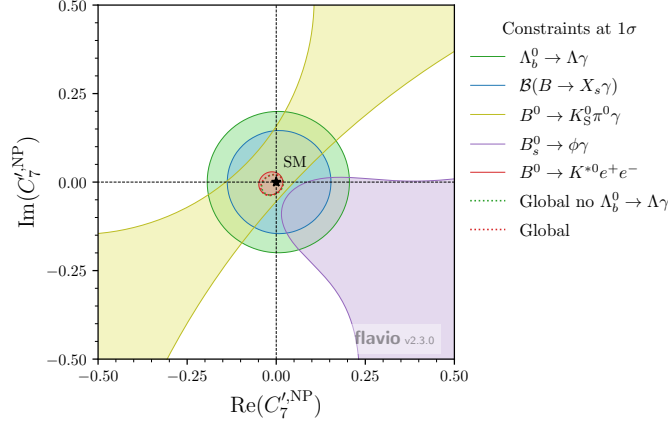


Figure 8: Experimental 1σ constraints on the size of NP contributions to C_7' . The strongest constraints arise from the LHCb measurements of $A_T^{(2)}$ and A_T^{Im} in the angular analysis of $B^0 \rightarrow K^{*0}e^+e^-$ decays [67] (red). Also shown are the constraints from: the LHCb measurement of the mixing-induced variables in $B_s^0 \rightarrow \phi\gamma$ decays [65] (purple); the LHCb direct measurement of the photon polarisation, α_γ , in $\Lambda_b^0 \rightarrow \Lambda\gamma$ decays [68] (green); the Belle measurement of the inclusive $B \rightarrow X_s\gamma$ branching fraction [72] (blue); the BaBar measurement of the mixing-induced CP asymmetry in $B^0 \rightarrow K_S^0\pi^0\gamma$ decays [73] (yellow). Figure obtained from Ref. [68].

fraction at $\mathcal{B}(\bar{E}_b \rightarrow \bar{E}^0\gamma) < 1.3 (0.6) \times 10^{-4}$ at 95% (90%) confidence level [69]. This limit is somewhat in tension with SM predictions based on light-cone sum rule calculations from Ref. [70]; however, it remains consistent with predictions from SU(3) flavour symmetry [71].

As shown in Fig. 8, the results discussed in this section can be translated into constraints on the size of NP contributions to C_7' . Currently, the $B^0 \rightarrow K^{*0}e^+e^-$ results are the most strongly constraining by far, and are in good agreement with the SM.

4. Global $b \rightarrow s\ell^+\ell^-$ fits

Measurements of $b \rightarrow s\ell^+\ell^-$ and $b \rightarrow s\gamma$ observables can be analysed in a model independent way through global fits defined in the WET approach, allowing the systematic assessment of possible NP scenarios. Historically, the results of such fits indicated that the available data was best described by models involving NP contributions to the $C_9^{(\prime)}$ and $C_{10}^{(\prime)}$ Wilson coefficients, which respectively describe the vector and axial-vector couplings of leptons to the effective weak interaction. Especially promising were scenarios involving LFU-violating contributions to $b \rightarrow s\mu^+\mu^-$ modes, *i.e.* to $C_{9\mu}^{(\prime)}$ and/or $C_{10\mu}^{(\prime)}$; although, marginally better descriptions of the data could be achieved by also including LFU-conserving contributions to $b \rightarrow se^+e^-$ and $b \rightarrow s\mu^+\mu^-$ modes [74].

The present status of global fits is, however, somewhat different. Importantly, the anomalies in $b \rightarrow s\mu^+\mu^-$ branching fractions and angular observables remain prominent and continue to favour NP models over the SM. However, the convergence of several key observables towards their SM values in recent experimental updates has interesting implications for the low-energy flavour structure of the aforementioned NP models. These effects are succinctly described in Ref. [35], with some of their key findings presented in Fig. 9. The scenario in which NP is allowed in $(C_{9\mu}, C_{10\mu})$

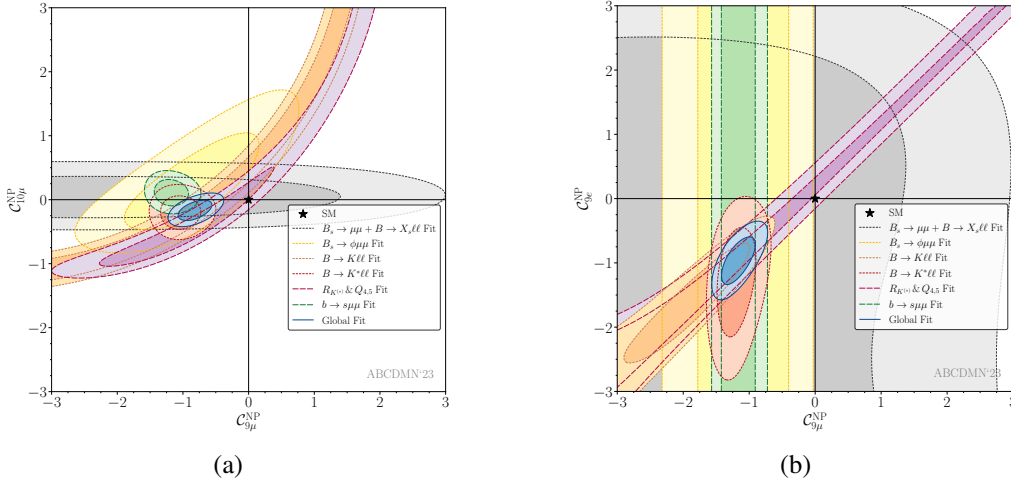


Figure 9: The present status of global fits to $b \rightarrow s\ell^+\ell^-$ observables. The reader is referred to Refs. [35, 74] for the full list of inputs. 1σ (dark shaded) and 2σ confidence regions are shown for two possible scenarios: (a) NP contributions are allowed to float in $(C_{9\mu}, C_{10\mu})$; (b) NP contributions are allowed to float in $(C_{9\mu}, C_{9e})$. Both scenarios are consistent with $C_{9\mu}^{\text{NP}} = -1$ at 1σ . In the second scenario, LFU conserving NP is preferred with $C_{9e}^{\text{NP}} = C_{9\mu}^{\text{NP}}$. This scenario provides the optimal fit to the data in the scenarios considered. Figure obtained from Ref. [35]

is shown in Fig. 9a. The global fit results indicate that significant NP contributions to $C_{10\mu}$ are no longer favoured to explain the data, which can be seen as a consequence of the new world average for $\mathcal{B}(B_s^0 \rightarrow \mu^+\mu^-)$. An alternative scenario in which NP is allowed in $(C_{9e}, C_{9\mu})$ is shown in Fig. 9b. Here, the results show that LFU-conserving NP in C_9 is now preferred, as opposed to LFU-violating NP in only $C_{9\mu}$. In fact, a NP contribution of $C_{9e}^{\text{NP}} = C_{9\mu}^{\text{NP}} \approx -1.0$ provides the best description of the data out of all scenarios considered, and is preferred over the SM at $> 5\sigma$ based on a χ^2 goodness of fit statistic. This is essentially a direct consequence of the latest LHCb results on R_K and R_{K^*0} , which expressly disfavour LFU violation. Evidently, however, the dynamical findings of $b \rightarrow s\ell^+\ell^-$ global fits over time show that yet more data and more theoretical advancements will be required to resolve the anomalies in $b \rightarrow s\ell^+\ell^-$ decays.

5. Conclusion

Decays involving $b \rightarrow s\{\gamma, e^+e^-, \mu^+\mu^-\}$ transitions have been the subject of intense study in recent years and continue to feed us tantalising hints of NP. Anomalous results have presented themselves in measurements of a number of observables, primarily in $b \rightarrow s\mu^+\mu^-$ decays. Until recently, the data generally favoured an explanation in terms of NP models involving LFU-violating contributions to $C_{9\mu}^{(\prime)}$ and/or $C_{10\mu}^{(\prime)}$; however, such models are now disfavoured in light of the recent R_K and R_{K^*0} results from LHCb. Additionally, updated measurements of $\mathcal{B}(B_s^0 \rightarrow \mu^+\mu^-)$ from CMS and LHCb leave little room for any NP in $C_{10\mu}^{(\prime)}$. Right-handed currents are disfavoured in view of the consistent SM agreement in $b \rightarrow s\gamma$ measurements. Taking all of this into consideration, global $b \rightarrow s\ell^+\ell^-$ fits indicate that a NP explanation indeed remains preferred over the SM at present, with the favoured scenario now being LFU-conserving contributions to C_9 . The overarching conclusion

to be drawn from these results is that continued study and enhancements in precision remain essential to resolving the $b \rightarrow s\ell^+\ell^-$ anomalies.

References

- [1] LHCb collaboration, R. Aaij *et al.*, *Measurement of Form-Factor-Independent Observables in the Decay $B^0 \rightarrow K^{*0}\mu^+\mu^-$* , *Phys. Rev. Lett.* **111** (2013) 191801, [arXiv:1308.1707](#).
- [2] LHCb collaboration, R. Aaij *et al.*, *Angular analysis of the $B^0 \rightarrow K^{*0}\mu^+\mu^-$ decay using 3fb^{-1} of integrated luminosity*, *JHEP* **02** (2016) 104, [arXiv:1512.04442](#).
- [3] LHCb collaboration, R. Aaij *et al.*, *Measurement of CP-averaged observables in the $B^0 \rightarrow K^{*0}\mu^+\mu^-$ decay*, *Phys. Rev. Lett.* **125** (2020) 011802, [arXiv:2003.04831](#).
- [4] LHCb collaboration, R. Aaij *et al.*, *Differential branching fraction and angular analysis of the $B^+ \rightarrow K^+\mu^+\mu^-$ decay*, *JHEP* **02** (2013) 105, [arXiv:1209.4284](#).
- [5] LHCb collaboration, R. Aaij *et al.*, *Test of lepton universality using $B^+ \rightarrow K^+\ell^+\ell^-$ decays*, *Phys. Rev. Lett.* **113** (2014) 151601, [arXiv:1406.6482](#).
- [6] LHCb collaboration, R. Aaij *et al.*, *Branching fraction measurements of the rare $B_s^0 \rightarrow \phi\mu^+\mu^-$ and $B_s^0 \rightarrow f_2'(1525)\mu^+\mu^-$ decays*, *Phys. Rev. Lett.* **127** (2021) 151801, [arXiv:2105.14007](#).
- [7] LHCb collaboration, R. Aaij *et al.*, *Test of lepton universality with $B^0 \rightarrow K^{*0}\ell^+\ell^-$ decays*, *JHEP* **08** (2017) 055, [arXiv:1705.05802](#).
- [8] LHCb collaboration, R. Aaij *et al.*, *Test of lepton universality in beauty-quark decays*, *Nature Physics* **18** (2022) 277, [arXiv:2103.11769](#).
- [9] J. Lyon and R. Zwicky, *Resonances gone topsy turvy - the charm of QCD or new physics in $b \rightarrow s\ell^+\ell^-$?*, [arXiv:1406.0566](#).
- [10] A. J. Buras, *Flavour Visions*, *PoS BEAUTY2011* (2011) 008, [arXiv:1106.0998](#).
- [11] K. De Bruyn *et al.*, *Branching Ratio Measurements of B_s Decays*, *Phys. Rev. D* **86** (2012) 014027, [arXiv:1204.1735](#).
- [12] M. Beneke, C. Bobeth, and R. Szafron, *Power-enhanced leading-logarithmic QED corrections to $B_q \rightarrow \mu^+\mu^-$* , *JHEP* **10** (2019) 232, [arXiv:1908.07011](#), [Erratum: *JHEP* **11**, 099 (2022)].
- [13] K. De Bruyn *et al.*, *Probing New Physics via the $B_s^0 \rightarrow \mu^+\mu^-$ Effective Lifetime*, *Phys. Rev. Lett.* **109** (2012) 041801, [arXiv:1204.1737](#).
- [14] LHCb collaboration, R. Aaij *et al.*, *Measurement of the $B_s^0 \rightarrow \mu^+\mu^-$ decay properties and search for the $B^0 \rightarrow \mu^+\mu^-$ and $B_s^0 \rightarrow \mu^+\mu^-\gamma$ decays*, *Phys. Rev.* **D105** (2022) 012010, [arXiv:2108.09283](#).
- [15] HFLAV collaboration, Y. S. Amhis *et al.*, *Averages of b-hadron, c-hadron, and τ -lepton properties as of 2018*, *Eur. Phys. J. C* **81** (2021) 226, [arXiv:1909.12524](#).

- [16] ATLAS collaboration, M. Aaboud *et al.*, *Study of the rare decays of B_s^0 and B^0 mesons into muon pairs using data collected during 2015 and 2016 with the ATLAS detector*, **JHEP** **04** (2019) 098, [arXiv:1812.03017](#).
- [17] CMS collaboration, A. M. Sirunyan *et al.*, *Measurement of properties of $B_s^0 \rightarrow \mu^+\mu^-$ decays and search for $B^0 \rightarrow \mu^+\mu^-$ with the CMS experiment*, **JHEP** **04** (2020) 188, [arXiv:1910.12127](#).
- [18] LHCb collaboration, R. Aaij *et al.*, *Measurement of the $B_s^0 \rightarrow \mu^+\mu^-$ branching fraction and effective lifetime and search for $B^0 \rightarrow \mu^+\mu^-$ decays*, **Phys. Rev. Lett.** **118** (2017) 191801, [arXiv:1703.05747](#).
- [19] LHCb collaboration, *Combination of the ATLAS, CMS and LHCb results on the $B_{(s)}^0 \rightarrow \mu^+\mu^-$ decays*, **LHCb-CONF-2020-002**, 2020, **ATLAS-CONF-2020-049**, **CMS PAS BPH-20-003**, **LHCb-CONF-2020-002**.
- [20] CMS collaboration, A. Tumasyan *et al.*, *Measurement of the $B_s^0 \rightarrow \mu^+\mu^-$ decay properties and search for the $B^0 \rightarrow \mu^+\mu^-$ decay in proton-proton collisions at $\sqrt{s} = 13$ TeV*, **Phys. Lett. B** **842** (2023) 137955, [arXiv:2212.10311](#).
- [21] T. Hurth, F. Mahmoudi, D. Martinez Santos, and S. Neshatpour, *Neutral current B-decay anomalies*, in *8th Workshop on Theory, Phenomenology and Experiments in Flavour Physics: Neutrinos, Flavor Physics and Beyond*, 2022, [arXiv:2210.07221](#).
- [22] LHCb collaboration, R. Aaij *et al.*, *Search for the rare decays $B_s^0 \rightarrow e^+e^-$ and $B^0 \rightarrow e^+e^-$* , **Phys. Rev. Lett.** **124** (2020) 211802, [arXiv:2003.03999](#).
- [23] LHCb collaboration, R. Aaij *et al.*, *Search for rare $B_{(s)}^0 \rightarrow \mu^+\mu^-\mu^+\mu^-$ decays*, **JHEP** **03** (2022) 109, [arXiv:2111.11339](#).
- [24] A. Bharucha, D. M. Straub, and R. Zwicky, *$B \rightarrow V\ell^+\ell^-$ in the Standard Model from light-cone sum rules*, **JHEP** **08** (2016) 098, [arXiv:1503.05534](#).
- [25] LHCb collaboration, R. Aaij *et al.*, *Measurement of the isospin asymmetry in $B \rightarrow K^*\mu^+\mu^-$ decays*, **JHEP** **07** (2012) 133, [arXiv:1205.3422](#).
- [26] LHCb collaboration, R. Aaij *et al.*, *Differential branching fractions and isospin asymmetries of $B \rightarrow K^{(*)}\mu^+\mu^-$ decays*, **JHEP** **06** (2014) 133, [arXiv:1403.8044](#).
- [27] LHCb collaboration, R. Aaij *et al.*, *Measurements of the S-wave fraction in $B^0 \rightarrow K^+\pi^-\mu^+\mu^-$ decays and the $B^0 \rightarrow K^*(892)^0\mu^+\mu^-$ differential branching fraction*, **JHEP** **11** (2016) 047, Erratum *ibid.* **04** (2017) 142, [arXiv:1606.04731](#).
- [28] LHCb collaboration, R. Aaij *et al.*, *Differential branching fraction and angular analysis of $\Lambda_b^0 \rightarrow \Lambda\mu^+\mu^-$ decays*, **JHEP** **06** (2015) 115, Erratum *ibid.* **09** (2018) 145, [arXiv:1503.07138](#).
- [29] LHCb collaboration, R. Aaij *et al.*, *Measurement of the $\Lambda_b^0 \rightarrow \Lambda(1520)\mu^+\mu^-$ differential branching fraction*, [arXiv:2302.08262](#), submitted to JHEP.

- [30] CMS collaboration, V. Khachatryan *et al.*, *Angular analysis of the decay $B^0 \rightarrow K^{*0}\mu^+\mu^-$ from pp collisions at $\sqrt{s} = 8$ TeV*, *Phys. Lett. B* **753** (2016) 424, [arXiv:1507.08126](#).
- [31] BELLE collaboration, S. Choudhury *et al.*, *Test of lepton flavor universality and search for lepton flavor violation in $B \rightarrow K\ell\ell$ decays*, *JHEP* **03** (2021) 105, [arXiv:1908.01848](#).
- [32] Belle collaboration, J.-T. Wei *et al.*, *Measurement of the Differential Branching Fraction and Forward-Backward Asymmetry for $B \rightarrow K^{(*)}\ell^+\ell^-$* , *Phys. Rev. Lett.* **103** (2009) 171801, [arXiv:0904.0770](#).
- [33] BaBar collaboration, J. P. Lees *et al.*, *Measurement of Branching Fractions and Rate Asymmetries in the Rare Decays $B \rightarrow K^{(*)}l^+l^-$* , *Phys. Rev. D* **86** (2012) 032012, [arXiv:1204.3933](#).
- [34] CDF collaboration, T. Aaltonen *et al.*, *Observation of the Baryonic Flavor-Changing Neutral Current Decay $\Lambda_b \rightarrow \Lambda\mu^+\mu^-$* , *Phys. Rev. Lett.* **107** (2011) 201802, [arXiv:1107.3753](#).
- [35] M. Algueró *et al.*, *To (b)e or not to (b)e: No electrons at LHCb*, [arXiv:2304.07330](#).
- [36] HPQCD collaboration, W. G. Parrott, C. Bouchard, and C. T. H. Davies, *Standard Model predictions for $B \rightarrow K\ell^+\ell^-$, $B \rightarrow K\ell^1-\ell^2+$ and $B \rightarrow K\nu\nu^-$ using form factors from $N_f=2+1+1$ lattice QCD*, *Phys. Rev. D* **107** (2023) 014511, [arXiv:2207.13371](#), [Erratum: *Phys.Rev.D* 107, 119903 (2023)].
- [37] N. Gubernari, M. Reboud, D. van Dyk, and J. Virto, *Improved theory predictions and global analysis of exclusive $b \rightarrow s\mu^+\mu^-$ processes*, *JHEP* **09** (2022) 133, [arXiv:2206.03797](#).
- [38] D. M. Straub, *flavio: a Python package for flavour and precision phenomenology in the Standard Model and beyond*, [arXiv:1810.08132](#).
- [39] R. R. Horgan, Z. Liu, S. Meinel, and M. Wingate, *Lattice QCD calculation of form factors describing the rare decays $B \rightarrow K^*\ell^+\ell^-$ and $B_s \rightarrow \phi\ell^+\ell^-$* , *Phys. Rev. D* **89** (2014) 094501, [arXiv:1310.3722](#).
- [40] R. R. Horgan, Z. Liu, S. Meinel, and M. Wingate, *Rare B decays using lattice QCD form factors*, *PoS LATTICE2014* (2015) 372, [arXiv:1501.00367](#).
- [41] S. Descotes-Genon and M. Novoa-Brunet, *Angular analysis of the rare decay $\Lambda_b \rightarrow \Lambda(1520)(\rightarrow NK)\ell^+\ell^-$* , *JHEP* **06** (2019) 136, [arXiv:1903.00448](#), [Erratum: *JHEP* 06, 102 (2020)].
- [42] Y.-S. Li, S.-P. Jin, J. Gao, and X. Liu, *Transition form factors and angular distributions of the $\Lambda_b \rightarrow \Lambda(1520)(\rightarrow NK)\ell^+\ell^-$ decay supported by baryon spectroscopy*, *Phys. Rev. D* **107** (2023) 093003, [arXiv:2210.04640](#).
- [43] Y. Amhis, M. Bordone, and M. Reboud, *Dispersive analysis of $\Lambda_b \rightarrow \Lambda(1520)$ local form factors*, *JHEP* **02** (2023) 010, [arXiv:2208.08937](#).

- [44] S. Meinel and G. Rendon, $\Lambda_c \rightarrow \Lambda^*(1520)$ form factors from lattice QCD and improved analysis of the $\Lambda_b \rightarrow \Lambda^*(1520)$ and $\Lambda_b \rightarrow \Lambda_c^*(2595, 2625)$ form factors, *Phys. Rev. D* **105** (2022) 054511, [arXiv:2107.13140](#).
- [45] J. Albrecht, D. van Dyk, and C. Langenbruch, *Flavour anomalies in heavy quark decays*, *Prog. Part. Nucl. Phys.* **120** (2021) 103885, [arXiv:2107.04822](#).
- [46] S. Descotes-Genon, J. Matias, M. Ramon, and J. Virto, *Implications from clean observables for the binned analysis of $B^- \rightarrow K^*\mu^+\mu^-$ at large recoil*, *JHEP* **01** (2013) 048, [arXiv:1207.2753](#).
- [47] CMS collaboration, A. M. Sirunyan *et al.*, *Measurement of angular parameters from the decay $B^0 \rightarrow K^{*0}\mu^+\mu^-$ in proton-proton collisions at $\sqrt{s} = 8$ TeV*, *Phys. Lett. B* **781** (2018) 517, [arXiv:1710.02846](#).
- [48] ATLAS collaboration, M. Aaboud *et al.*, *Angular analysis of $B_d^0 \rightarrow K^*\mu^+\mu^-$ decays in pp collisions at $\sqrt{s} = 8$ TeV with the ATLAS detector*, *JHEP* **10** (2018) 047, [arXiv:1805.04000](#).
- [49] Belle collaboration, S. Wehle *et al.*, *Lepton-Flavor-Dependent Angular Analysis of $B \rightarrow K^*\ell^+\ell^-$* , *Phys. Rev. Lett.* **118** (2017) 111801, [arXiv:1612.05014](#).
- [50] A. Khodjamirian, T. Mannel, A. A. Pivovarov, and Y.-M. Wang, *Charm-loop effect in $B \rightarrow K^{(*)}\ell^+\ell^-$ and $B \rightarrow K^*\gamma$* , *JHEP* **09** (2010) 089, [arXiv:1006.4945](#).
- [51] S. Descotes-Genon, L. Hofer, J. Matias, and J. Virto, *On the impact of power corrections in the prediction of $B \rightarrow K^*\mu^+\mu^-$ observables*, *JHEP* **12** (2014) 125, [arXiv:1407.8526](#).
- [52] LHCb collaboration, R. Aaij *et al.*, *Angular analysis of the $B^+ \rightarrow K^{*+}\mu^+\mu^-$ decay*, *Phys. Rev. Lett.* **126** (2021) 161802, [arXiv:2012.13241](#).
- [53] CMS collaboration, A. M. Sirunyan *et al.*, *Angular analysis of the decay $B^+ \rightarrow K^*(892)^+\mu^+\mu^-$ in proton-proton collisions at $\sqrt{s} = 8$ TeV*, *JHEP* **04** (2021) 124, [arXiv:2010.13968](#).
- [54] LHCb collaboration, R. Aaij *et al.*, *Angular analysis and differential branching fraction of the decay $B_s^0 \rightarrow \phi\mu^+\mu^-$* , *JHEP* **09** (2015) 179, [arXiv:1506.08777](#).
- [55] LHCb collaboration, R. Aaij *et al.*, *Angular analysis of the rare decay $B_s^0 \rightarrow \phi\mu^+\mu^-$* , *JHEP* **11** (2021) 043, [arXiv:2107.13428](#).
- [56] LHCb collaboration, R. Aaij *et al.*, *Angular analysis of charged and neutral $B \rightarrow K\mu^+\mu^-$ decays*, *JHEP* **05** (2014) 082, [arXiv:1403.8045](#).
- [57] CMS collaboration, A. M. Sirunyan *et al.*, *Angular analysis of the decay $B^+ \rightarrow K^+\mu^+\mu^-$ in proton-proton collisions at $\sqrt{s} = 8$ TeV*, *Phys. Rev. D* **98** (2018) 112011, [arXiv:1806.00636](#).
- [58] LHCb collaboration, R. Aaij *et al.*, *Angular moments of the decay $\Lambda_b^0 \rightarrow \Lambda\mu^+\mu^-$ at low hadronic recoil*, *JHEP* **09** (2018) 146, [arXiv:1808.00264](#).
- [59] C. Bobeth, G. Hiller, and G. Piranishvili, *CP Asymmetries in $\bar{B} \rightarrow \bar{K}^*(\rightarrow \bar{K}\pi)\bar{\ell}\ell$ and Untagged $\bar{B}_s, B_s \rightarrow \phi(\rightarrow K^+K^-)\bar{\ell}\ell$ Decays at NLO*, *JHEP* **07** (2008) 106, [arXiv:0805.2525](#).

- [60] LHCb collaboration, R. Aaij *et al.*, *Tests of lepton universality using $B^0 \rightarrow K_S^0 \ell^+ \ell^-$ and $B^+ \rightarrow K^{*+} \ell^+ \ell^-$ decays*, *Phys. Rev. Lett.* **128** (2022) 191802, [arXiv:2110.09501](#).
- [61] LHCb collaboration, R. Aaij *et al.*, *Test of lepton universality using $\Lambda_b^0 \rightarrow p K^- \ell^+ \ell^-$ decays*, *JHEP* **05** (2020) 040, [arXiv:1912.08139](#).
- [62] LHCb collaboration, R. Aaij *et al.*, *Measurement of lepton universality parameters in $B^+ \rightarrow K^+ \ell^+ \ell^-$ and $B^0 \rightarrow K^{*0} \ell^+ \ell^-$ decays*, [arXiv:2212.09153](#), to appear in *Phys. Rev. D*.
- [63] LHCb collaboration, R. Aaij *et al.*, *Test of lepton universality in $b \rightarrow s \ell^+ \ell^-$ decays*, [arXiv:2212.09152](#), to appear in *Phys. Rev. Lett.*
- [64] F. Muheim, Y. Xie, and R. Zwicky, *Exploiting the width difference in $B_s \rightarrow \phi \gamma$* , *Phys. Lett. B* **664** (2008) 174, [arXiv:0802.0876](#).
- [65] LHCb collaboration, R. Aaij *et al.*, *Measurement of CP-violating and mixing-induced observables in $B_s^0 \rightarrow \phi \gamma$ decays*, *Phys. Rev. Lett.* **123** (2019) 081802, [arXiv:1905.06284](#).
- [66] LHCb collaboration, R. Aaij *et al.*, *Measurement of the ratio of branching fractions $\mathcal{B}(B^0 \rightarrow K^{*0} \gamma) / \mathcal{B}(B_s^0 \rightarrow \phi \gamma)$ and the direct CP asymmetry in $B^0 \rightarrow K^{*0} \gamma$* , *Nucl. Phys.* **B867** (2013) 1, [arXiv:1209.0313](#).
- [67] LHCb collaboration, R. Aaij *et al.*, *Strong constraints on the $b \rightarrow s \gamma$ photon polarisation from $B^0 \rightarrow K^{*0} e^+ e^-$ decays*, *JHEP* **12** (2020) 081, [arXiv:2010.06011](#).
- [68] LHCb collaboration, R. Aaij *et al.*, *Measurement of the photon polarization in $\Lambda_b^0 \rightarrow \Lambda \gamma$ decays*, [arXiv:2111.10194](#), submitted to PRL.
- [69] LHCb collaboration, R. Aaij *et al.*, *Search for the radiative $\Xi_b^- \rightarrow \Xi^- \gamma$ decay*, *JHEP* **01** (2022) 069, [arXiv:2108.07678](#).
- [70] Y.-l. Liu, L.-f. Gan, and M.-q. Huang, *The exclusive rare decay $b \rightarrow s \gamma$ of heavy b-Baryons*, *Phys. Rev. D* **83** (2011) 054007, [arXiv:1103.0081](#).
- [71] R.-M. Wang *et al.*, *Studying radiative baryon decays with the SU(3) flavor symmetry*, *J. Phys. G* **48** (2021) 085001, [arXiv:2008.06624](#).
- [72] Belle collaboration, Y. Ushiroda *et al.*, *Time-Dependent CP Asymmetries in $B^0 \rightarrow K_S^0 \pi^0 \gamma$ transitions*, *Phys. Rev. D* **74** (2006) 111104, [arXiv:hep-ex/0608017](#).
- [73] BaBar collaboration, B. Aubert *et al.*, *Measurement of Time-Dependent CP Asymmetry in $B^0 \rightarrow K_S^0 \pi^0 \gamma$ Decays*, *Phys. Rev. D* **78** (2008) 071102, [arXiv:0807.3103](#).
- [74] M. Algueró *et al.*, *$b \rightarrow s \ell^+ \ell^-$ global fits after R_{K_S} and $R_{K^{**}}$* , *Eur. Phys. J. C* **82** (2022) 326, [arXiv:2104.08921](#).